J. Membrane Biol. 155, 263–274 (1997)

The Journal of
Membrane
Biology

The Actions of Calmodulin Antagonists W-7 and TFP and of Calcium on the Gating Kinetics of the Calcium-activated Large Conductance Potassium Channel of the *Chara* Protoplasmic Drop: A Substate-sensitive Analysis

D.R. Laver[1], C.A. Cherry[2]*, N.A. Walker[2]*

[1]Division of Neuroscience, John Curtin School of Medical Research, Australian National University, Canberra, ACT 2601, Australia
[2]The biophysics Laboratory, School of Biological Sciences, University of Sydney, NSW 2006, Australia

Received: 26 August 1996/Revised: 7 October 1996

Abstract. The effects of the calmodulin antagonists W-7 and trifluoperazine have been measured on the Ca^{2+}-activated potassium channel in the membrane surrounding protoplasmic drops expressed from internodal cells of charophyte plants. The large-conductance (170 pS), voltage- and Ca^{2+}-dependent gating, and prominent conductance substrate of this channel shows a strong kinetic resemblance to those of the Maxi-K channel from animal cells.

This is the first study of the action of calmodulin antagonists which measures their effects on the most populated substates as well as the closed and main open states of Maxi-K channels. The substate analysis provides new evidence for different modes of action of- and different bindings sites for these calmodulin antagonists.

Neither antagonist produces the simple closure of the channel reported previously as its effect on the Maxi-K channel, though both do induce flicker-block, reducing the mean current to near zero at high concentrations following an inverted Michaelis-Menten curve.

W-7 reduces residence time in the fully open state, thus raising, in the same proportions, the probabilities of finding the channel in the closed state or a pre-existing substate. Its binding to the channel is voltage- and calcium-dependent.

In contrast, trifluoperazine reduces residence in the open state and promotes an apparently new substate which overlaps the closed state at −50 mV but is distinguishable from it at voltages more negative than −100 mV. This substate may represent times that trifluoperazine is bound to the channel.

Both antagonists have effects clearly distinguishable from that of withdrawing calcium from the channel, which does not affect open state residence time but increases closed state residence time. Thus neither antagonist reverses the activating effect of Ca^{2-}. This is good kinetic evidence against the view that the channel is activated by Ca^{2+}-calmodulin and that the effect of a calmodulin antagonist is to reverse this process by making Ca^{2-}-calmodulin less available.

Key words: Calmodulin — Maxi-K channel — Charophyte — Trifluoperazine — W-7

Introduction

The membrane surrounding protoplasmic drops expressed from internodal cells of charophyte plants shows channel activity, most obviously that of a calcium-activated large-conductance (170 pS) potassium channel. This has been an object of study since Lühring (1986) reported on its K^+ selectivity, bursting kinetics and voltage activation and on its having a conductance substate. The protoplasmic drop membrane originates largely from the tonoplast (vacuole membrane) (Lühring, 1986; Sakano & Tazawa, 1986) and the channels it contains are believed to reside in the tonoplast *in vivo.*

The gating kinetics of the channel have been studied by Laver and Walker (1987) who confined their attention to the modeling of closed and fully open conduction states, ignoring states of submaximal conductance. As extended and modified by Laver (1990, 1992) the resulting kinetic model has one open state and two gating mechanisms with opposite voltage dependence. In addition, channel closures produced by calcium on either the cytoplasmic or the vacuolar side of the patch, are ex-

* *Correspondence to:* D.R. Laver

plained in terms of the Woodhull (1973) model of voltage-dependent block (Laver, 1990, 1992).

The existence of a number of conduction substates was demonstrated for the present channel by Tyerman et al. (1992). They showed that the most populated substate, which they called the 'midstate', had a lower conductance than the main open state and that it has a superlinear *I/V* curve while the main conductance state has a sublinear *I/V* curve. They showed that the half-amplitude detection method of Colquhoun and Sigworth (1983), which ignores substates is inappropriate for analyzing gating kinetics of the maxi-K channel. The existence of subconductance states is taken into account in the present analysis.

In its selectivity, gating kinetics and conduction characteristics, the present charophyte Maxi-K (C-Maxi-K) channel closely resembles the animal maxi-K (A-Maxi-K) channel (Laver & Walker, 1991; Laver, 1992). Although, unlike most A-Maxi-K channels, the C-Maxi-K is not blocked by CTX (D. Laver, *unpublished results*) it is inhibited by eflurane (Antkowiak & Kirshfield, 1992). It has been suggested that the calcium-activated potassium channel of *Chenopodium rubrum* tonoplast (SV) is related to the A-Maxi-K channel (Weiser & Bentrup, 1993), largely on the basis of its pharmacology. The SV channel, like most A-Maxi-K channels, is inhibited by CTX and not by apamine: however its low unitary conductance and its low selectivity argue for caution in accepting this relationship especially as its kinetics have not been critically studied.

Like the A-Maxi-K channel (Blatz & Magleby, 1987) and the plant SV channel (Hedrich & Neher, 1987), the C-Maxi-K is activated by calcium on the cytoplasmic side (Laver & Walker, 1991) at a level (1 μM) above that expected in the normal, unexcited cell, but likely during an action potential (Williamson & Ashley, 1982). Fluxes of potassium from vacuole to cytoplasm which occur during the action potential are presumed to be mediated by the C-Maxi-K channel (Laver & Walker, 1991).

Calmodulin (CAM) frequently mediates calcium activation and it has been reported as binding to the A-Maxi-K channel from renal medulla (Klaerke, Peterson & Jorgensen 1987). It has not been shown to mediate calcium activation in A-Maxi-K channels of dog airway smooth muscle (McCann & Welsh, 1987) and of rat myometrium (Kihira et al., 1990), discussed further below. Investigators of some other calcium-activated ion channels have concluded that the calcium activation is mediated by CAM. Potassium channels are reported to be calcium-CAM-1 activated in a number of cells including neurones (Onozuka et al., 1987) and *Paramecium* (Hinrichsen et al., 1986). Calcium-activated channels in plant cells, notably the vacuolar SV (Weiser, Blum & Bentrup, 1991; Bethke and Jones, 1994) and the charophyte plasma membrane chloride channel (Okihara, Ohkawa & Kasai, 1991), have been claimed to be calcium-CAM-activated. The question of CAM-mediation of calcium-activation has not previously been addressed for the C-maxi-K channel.

The present study arose from the search for a ligand that might be used for identification and purification of the C-maxi-K channel protein; it developed into an inquiry into the pharmacology of the channel, and the mechanism of the action of CAM antagonists, specifically W-7 and TFP.

W-7 and TFP are widely-used CAM antagonists (Hidaka et al., 1981; Roufogalis, 1982). The mechanism of their CAM antagonism is unclear: it has been proposed that antagonists interact with the hydrophobic regions of the Ca-CAM complex which become exposed during the conformational change it undergoes as a result of binding with calcium (Shatzman, Raynor & Tazawa, 1983). These hydrophobic regions are located in clefts in the globular regions of the dumbbell and appear crucial to the activation of the complex. More importantly for our present purpose, it has been clear since early work on W-7 that it inactivates calcium-activated proteins that are not CAM-dependent (Shatzman et al., 1983; Roufogalis, 1982), so that it and other CAM antagonists are not specific probes for CAM action, although often used in this role.

Investigations of CAM antagonists' action on Ca^{2+}-activated channels have been many, mostly fairly perfunctory. In a careful study of A-Maxi-K channels of dog airway smooth muscle, McCann and Welsh (1987) showed that the CAM antagonists TFP, CPR, TRZ and HPD all reduced open probability and mean open duration at micromolar concentrations, and that their affinities (HPD > TFP > CPM > TRZ) were not in the same order as their affinities for antagonizing CAM action (TFP > CPM > HPD). They modeled the kinetic effects as simple block of the channel by the antagonist, and suggested that the antagonists act directly on the channel, not via CAM. The effects of W-5, W-7 and TFP on the activity of the A-maxi-K channel from pregnant rat myometrium were studied by Kihira et al. (1990). They stated that all three produced the same effects, and showed that W-7 reduced the long (calcium-dependent) time constant in the open time distribution without a consistent effect on the distribution of closed times, and that W-7 did not affect the calcium concentration needed for half-activation of the channel. They concluded therefore that the effects of CAM antagonists were the result of direct binding to the channel rather than of an inhibition of CAM action. These analyses used versions of the half-amplitude method, ignoring the existence of a substate which had been established for the A-Maxi-K channel (Barrett, Magelby & Pallotta, 1982). However an inspection of the records shown by Barrett et al. (1982)

suggests that the substate (at 40% of the open-state amplitude at −30 mV) may occur more often than the claimed once in 1000–10,000 openings, and that ignoring it may therefore lead to errors in analysis.

We report here the first study of the effects of the antagonists W-7 and TFP on a Maxi-K channel using appropriate analysis methods for a channel exhibiting conductance substates; we will show that such analysis can distinguish between their effects and can offer a pointer towards their different modes of action.

Materials and Methods

Solutions and Solution Exchange

We used solutions of the following compositions (In mM): *Bath Solution:* 150 KCl, 1 $CaCl_2$, 10 HEPES, pH 7.3; *Low Calcium Bath Solution:* 150 KCl, 870 μM $CaCl_2$, 1 EGTA (=1 μM free calcium), 10 HEPES, pH 7.3; *Pipette Solution:* 50–500 KCl, 1 $CaCl_2$, 10 MES pH 5.6; *Calmodulin Solution:* 150 KCl, 870 μM $CaCl_2$, 1 EGTA (=1 μM free calcium), 10 HEPES, 9–90 NM spinach CAM, pH 7.3 (CAM was also tested at 0.1 μM Ca^{2+}); *W-7 Solution:* 150 KCl, 870 μM $CaCl_2$, 1 EGTA (=1 μM free calcium), 10 mM HEPES, 50 μM W-7, pH 7.3.

The concentration of free calcium was calculated using the BUFFA program (courtesy of R.G. Ryall, Flinders Medical Research Centre). Spinach CAM (Sigma-Aldrich) has a 86% identity with *Chlamydomonas* CAM and 97–99% identity with other higher plant CAMs (Roberts & Harmon, 1992). W-7 (Sigma-Aldrich) solution was made up the day before the experiment. It was dissolved in Low-Calcium bath solution, stirred for 2 hr and left to dissolve overnight at room temperature. All solutions were adjusted to the appropriate pH using KOH.

Bath solutions were altered using two protocols (1) W-7 was applied using perfusion of the bath solution. Solution (10 ml) was cycled through the 3 ml bath using a back-to-back dual syringe system. W-7 was then removed from solution by perfusing with fresh Bath Solution containing additional CAM. Channel activity was constantly monitored during these changes of solution. Activity was then measured for a further 1–2 min to follow the recovery of activity. (2) Inhibitors were also applied directly to the bath solution using a micropipette, which was also used to mix the bath.

Patch Pipettes

Borosilicate microcapillary tubing was used to make pipettes. A two-stage pull on a vertical electrode puller (Kopf Model 720) was used to obtain pipettes with tip resistance about 30 MΩ. Pipette tips were fire-polished but coating with Sylgard™ was not necessary as patches were excised and always brought to the level just below the surface of the bath medium, diminishing pipette surface noise. For a more detailed description of the manufacture of pipettes see Laver and Walker (1987).

Cytoplasmic Droplets

Internodal cells of *Chara australis* R.Br. were cut from the plant and kept in normal growing solution 16 hr before experimental use. Cells were blotted dry 2 min before use, and then one end was cut off. The contents of the cell were expressed using rubber coated tweezers into Bath solution following the method of Kamiya and Kuroda (1957). Cytoplasmic droplets formed almost instantly. For consistency, droplets about 20 μm in diameter were selected for experimental use. The droplet preparations were viable for 1 hr only. After this time, membranes started visibly to break down and seals were noisy: such records are not included in the analysis presented here. High resistance seals (10–50 Gω) formed when suction was applied. The pipette was withdrawn from the membrane, usually detaching an inside-out patch. When a vesicle was present the pipette tip was moved through the air-water interface to break it.

Electrical Measurements

Potential differences across membrane patches are all expressed according to standard convention; positive current represents the movement of positive charge from the cytoplasmic side to the vacuolar side of the membrane (outward current) and voltage is with respect to the vacuole as ground. When seals were formed, patches were voltage-clamped over the voltage range −50 to −200 mV, over which activity was present. Seals were often unstable at voltages more negative than −150 mV, so data quoted mainly covers the range −50 to −150 mV. Although most records were taken from single-channel patches, it was commonly observed that large-conductance K^+ channels may stay dormant for a long period, and reappear spontaneously. Records with this type of activity were not used for open probability measurements. All measurements were taken after channel activity was judged to have reached a stable condition, based on measurements of P_o (*see below*). All experiments were carried out at 22 ± 2°C.

Data Recording and Analysis

Two patch rigs were used. In Sydney the amplifier was a List Model EPC7; membrane current was displayed on a Gould digital storage oscilloscope (Model 1421), and recorded using a Sony Betamax video recorder in conjunction with a Sony Pulse Code Modulator (Model 501-ES). In Canberra the amplifier was an Axon Instruments Axopatch (Model 200A), the membrane current was displayed on a Hitachi Digital Storage Oscilloscope and recorded on videotape using pulse code modulation (Model 200 from A.R. Vetter). For analysis the replayed records were filtered at 10 kHz using a 4 pole low-pass Bessel filter, sampled at 20 kHz and digitized using a 12-bit AD/DA board (Data Translation Model DT2801A or Tecmar Model TL-1). The sample rate of twice the filter corner frequency is needed to eliminate correlations between neighboring data points, a requirement of the HMM analysis algorithm (*see below*). Preliminary analysis was carried out using the software package CHANNEL II (courtesy Michael Smith, John Curtin School of Medical Research, Australian National University). CHANNEL II was used to produce hard copies of raw data records (filtered where appropriate with a running average filter) and to analyze mean currents, amplitudes and open time probabilities. More detailed analysis of the mechanism of the block by W-7 and TFP was carried out using two analytical methods. Channel gating kinetics were recovered from the background noise using the programme HMM (Hidden Markov Model), from S. Chung, Department of Chemistry, Australian National University (Chung et al., 1990, 1991) or EVPROC, developed by D.R. Laver (Kourie et al. 1996).

The programme HMM finds the maximum likelihood estimate of the transitions present in the record and provides for the identification of substate levels and the determination of state amplitude, open probability and transition probability. It is based on the assumption that the signal is the sum of a first order finite state Markov process and white,

uncorrelated, Gaussian noise of known variance. We began HMM analysis by deciding the number of current levels in the original signal: a maximum-likelihood amplitude histogram was produced (using Option #6); the number of unknown levels and their approximate positions were deduced from the amplitude histogram, and the programme (using Option #2) locates the levels and provides the transition matrix; once the levels were known we could obtain the maximum-likelihood estimate of the original signal (using Option #1). While HMM uses probably the most sensitive analysis technique yet applied to single channel recordings it computationally expensive. This makes its use impractical for records in which substates occur infrequently, as they do in those from the C-Maxi-K channel (Tyerman et al., 1992). So HMM analysis was complemented by use of the programme EVPROC, which uses a faster, less rigorous method of detecting transitions. The method is based on the assumption that the signal is the sum of a series of stepwise process, transitions are accepted if they exceed a variable threshold; if not, the adjacent levels are replaced by their weighted mean. The threshold (T) is determined by the variance of the noise (s^2) and the number (n) of samples in the shortest level adjacent to the transition:

$$T = A \cdot s/\sqrt{n} \quad (1)$$

where $s/\sqrt{n}$ is the standard error of the estimate of the current level. We set $A = 2$ so that the accepted transitions have a significance >95%.

In the figures shown we used an average of 5 patch records in obtaining mean current data. The combined white noise recorded in this system was <1 pA RMS with a bandwidth of 10 kHz. Records presented were filtered with a running average-of-5 filter.

Data are presented first as open probability, P_o, measured directly as within-burst mean current divided by unitary current. This statistic is a convenient summary, but it is recognized that for a channel with more than one conductance state it has no precise meaning. In presenting later the results of analysis by HMM or EVPROC we can deal with estimates of transition probabilities, event probabilities and event durations, whose meanings are well-defined if the states to which they refer are well-defined. The channel shows a distribution of closed states that includes some very long durations, so that it is not practicable to measure open probability over whole records. We define bursts as periods of activity separated by closed durations of 1 sec or more.

Abbreviations

CAM (calmodulin):	Phosphodiesterase 3′-5′-cyclic nucleotide activator
CPZ (chlorpromazine):	2-Chloro-N,N-dimethyl-10H-phenothiazine-10-propanomine
CTX:	Charybdotoxin
HPD (haloperidol):	4-[4-(4-Chlorophenyl)-4-dihydroxypiperidinyl]-1-(4-fluorophenyl)-1-butanone
TFP (trifluoperazine):	10-[3-(4-Methyl-1-piperazinyl)propyl]-2-(trifluoromethyl)-10H-phenothiazine
TRZ (thioridazine):	10-[2-(1-Methyl-2-piperidinyl)ethyl]h-2-(methylthio)-10H-phenothiazine
W-5:	N-6-aminohexyl)-1-napthalene sulfonamide
W-7:	N-6-(aminohexyl)-5-chloro-1-napthalene sulfonamide

Results

General Observations of Effects of CAM Antagonists

Flicker Block

Both W-7 and TFP produced concentration-dependent block at micromolar concentrations, on the cytoplasmic side of the membrane, causing flickering channel activity and a slightly reduced amplitude (Fig. 1), each flicker representing a very fast channel closure. This flicker block is analyzed in the present paper. The block was reversible partly or fully, the channel recovering 60% to 100% of its mean current after removal of blocking agent. Careful inspection suggests that the effects of W-7 and TFP are different (Fig. 1), and such a difference appears more clearly during the analysis below.

Effects of Cytoplasmic Calcium and Membrane PD on Flicker Block by W-7

The effect of W-7 on open probability fits a Michaelis-Menten relationship; Figure 2 shows an experiment in 10 μM Ca^{2+} in which, as was typical, the data could be fitted with a Michaelis-Menten inhibition curve falling to zero open probability at infinite W-7 concentration, and in this case with K_i of 11 μM. The median values from 24 such experiments were fitted by weighted least squares to give the following values of K_i (±standard error):

$[Ca^{2+}]$/μM	K_i/μM
1	2.5 ± 0.7
10	16 ± 4.5
1000	11 ± 2.0

There was marked variability in K_i between different patches. This variability in apparent binding constant is found also with TFP and Ca^{2+}. Calcium reduces W-7 binding but does not reduce it to zero at high concentrations. This is not a simple competitive interaction; it would be consistent with a binding site with micromolar affinity for Ca^{2+} which partially destabilizes W-7 binding.

Similar experiments showed that the effect of W-7 on open probability was voltage-dependent, the apparent K_i being:

PD/mv	K_i/μM
0	17 ± 1
−50	25 ± 3
−80	61 ± 4

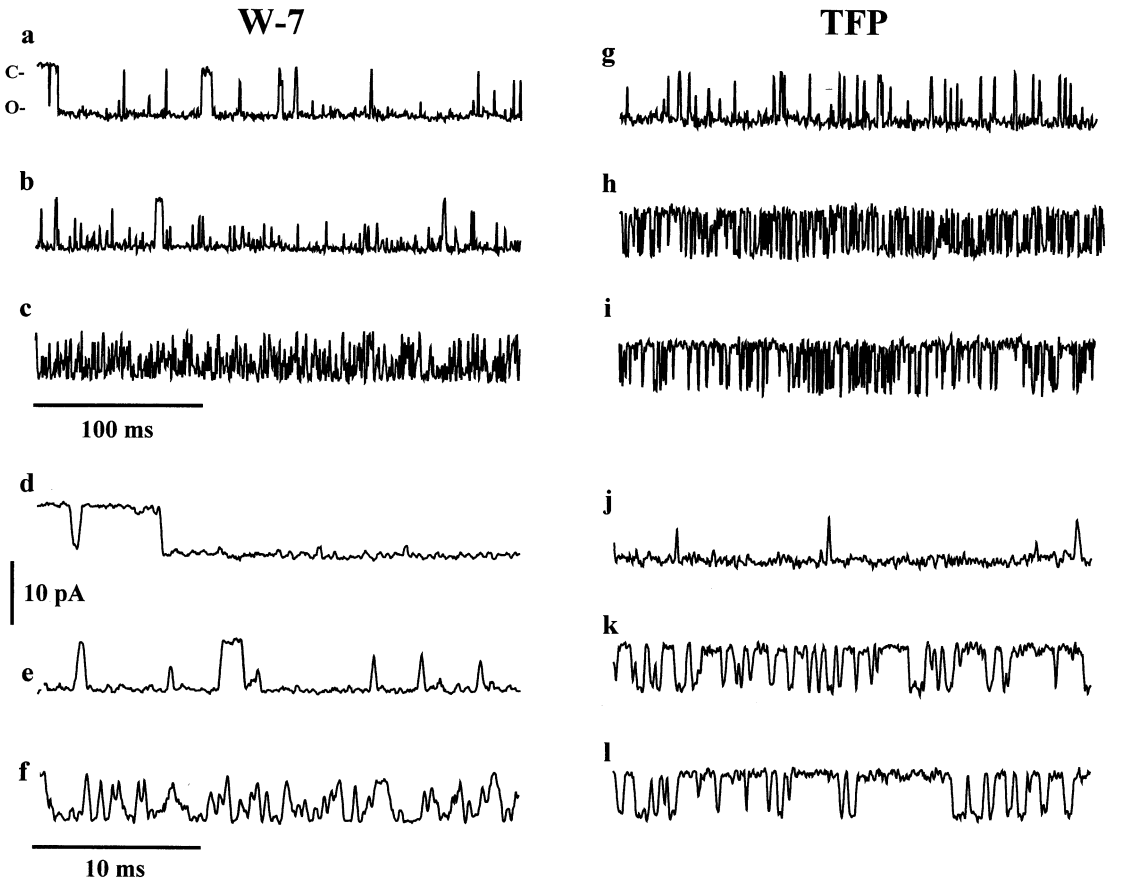

Fig. 1. Digitized records of the large-conductance K^+ channel in excised inside-out patches of *Chara* cytoplasmic droplets, at −50 mV, in 1 mM Ca^{2+}, in various [W-7] and [TFP]. Channel openings are shown as downward current steps. Filtered by running average of 5. Concentrations are: (*a*) control; (*b*) 8.2 μM W-7; (*c*) 30 μM W-7; (*d*) control; (*e*) 8.2 μM W-7; (*f*) 30 μM W-7; (*g*) control; (*h*) 8.2 μM TFP; (*i*) 16.3 μM TFP; (*j*) control; (*k*) 8.2 μM TFP; (*l*) 16.3 μM TFP. Experiments dc239 and dc327.

Analysis of Flicker Block by W-7

Figure 3 shows the maximum likelihood estimate of the amplitude histogram, as generated by HMM from a record at −50 mV for a patch in symmetrical 150 mM KCl with 1 μM $CaCl_2$ on the cytoplasmic face and 1 mM $CaCl_2$ on the vacuolar face. Distinct conductance levels are seen as peaks in this distribution. The effect of W-7 was to decrease the probability of the highest channel conductance state. This decrease in probability appeared to be absorbed by the lower conductance levels. A more precise determination of the amplitudes and probabilities the channel conductance states was found using the four-state HMM analysis (*see* below).

For a channel at −50 mV in symmetric 150 mM KCl and 1 mM $CaCl_2$ the mean duration of levels as a function of their amplitude and of [W-7] is shown in Fig. 4. The control record had too few events to give a statistically significant representation of the duration, so in constructing this figure a record from another channel was added. The mean durations for closed, open and midstates are longer than 100 μs, while the mean durations of the other levels are shorter than 50 μs. It is clear that W-7 decreases only the open state mean duration, which results in the reduced open state probability noted above.

Four-state Analysis

The arrows at the top of Fig. 3 indicate levels consistently chosen as the maximum likelihood estimates by HMM with the assumption that there are 4 levels. The lowest of these chosen levels corresponds to the closed state, the highest to the open state, and the level at about 2 pA to the midstate described by Tyerman *et al.* (1992). Amplitude distributions generated by HMM and by EVPROC also indicate the presence of a range of less easily-defined substates. When HMM searched under the assumption of 4 levels the closed, open and midstate levels were well-defined, i.e., consistently chosen at

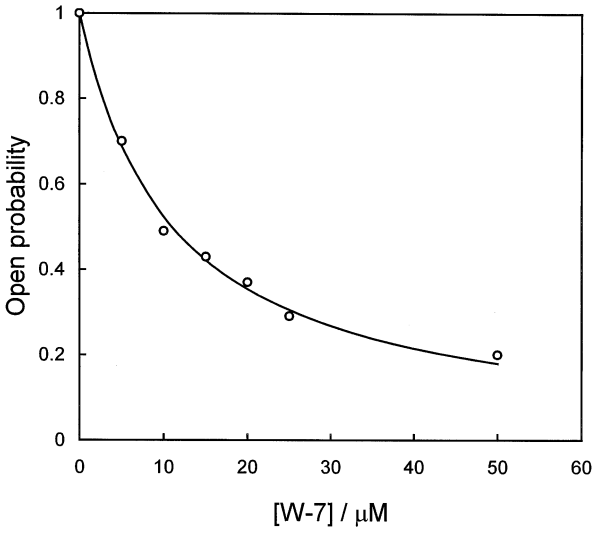

Fig. 2. Effect of W-7 on open probability within bursts (*see* text) relative to that at zero [W-7] in 10 μM Ca^{2+}. Fitted line: Michaelis-Menten curve falling to zero at infinite [W-7], with K_i of 11 μM. Experiment 55w7.

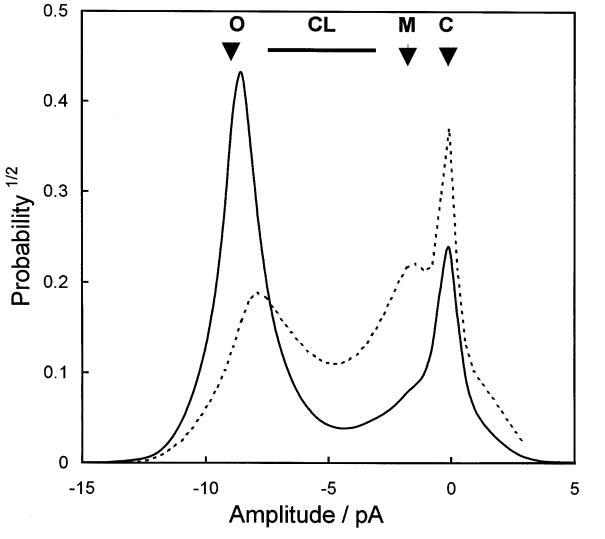

Fig. 3. Effect of W-7 on the amplitudes of C-maxi-K channels at −50 mV in 1 μM Ca^{2+} (Experiment 67w7, representative of seven experiments). Maximum likelihood amplitude histogram generated from HMM (using Option #6). The W-7 concentrations are: (solid line) zero; (dotted line) 8.3 μM. Solid arrows mark 3 amplitudes consistently chosen by HMM (using Option #2, assuming 4 levels) and labelled as, left to right: (O) open state; (M) midstate and (C) closed state. The bar marks a range in which HMM chooses the fourth amplitude, representing what appeared to be a cluster of short-lived states, labeled: (CL) cluster state.

close to the same positions, while the position of the fourth level varied considerably, even between different sections of the same record. The bar in Fig. 3 indicates the range of these choices. We take it that this range

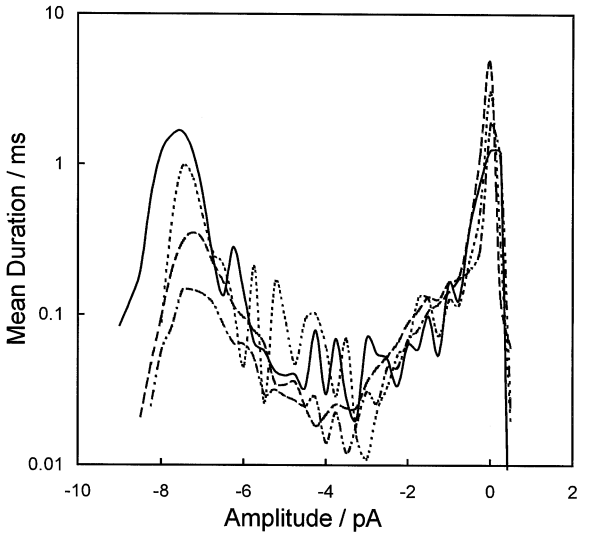

Fig. 4. Mean event duration as a function of amplitude and W-7 concentration over the range 8 to 80 μM in symmetrical 1 mM Ca^{2+} derived from EVPROC analysis (Experiment dc239 shown here is representative of seven experiments). The mean durations were derived from the ratio of the number of data points and the number of channel openings at each amplitude. The W-7 concentrations are: (full line) 8.2 μM; (dotted line) 16 μM; (dashed line) 32 μM; (dashes and dots) 77 μM. The control record in zero [W-7] had too few channel openings for a good measurement of mean durations; the control was similar to the data obtained at 8 μM W-7.

contains a (possibly large) number of lightly populated, short-lived states: the difficulty in defining their levels is their short duration (shown below). Because it is impractical to characterize these sparsely populated levels separately we have often used HMM with the assumption that there are four conductance levels, with one single level available to represent the many sparse states.

The effect of W-7 on the amplitudes of the 4 states is shown in Fig. 5—the open-state and midstate currents are unaffected by W-7, while the upper substate is very variable but shows no significant effect. The current-voltage characteristics of open and mid states are shown in Fig. 6, in the absence and presence of W-7 in symmetric 150 mM KCl plus 1 mM $CaCl_2$. Again W-7 has no significant effect on amplitudes over a wide range of concentration and PD. The conductances of open state and midstate appear to be unaffected or slightly reduced by W-7, and the large reduction in mean current it produces is mainly due to a reduction in open state duration and probability (*see below*). Associated with this reduction is an increase in the probabilities of the closed state and the substates.

Figure 7 shows the effect of W-7 on the substate probabilities and mean durations. W-7 causes a decrease in the main state probability which is absorbed by proportional increases in the other three states (Fig. 7*A*).

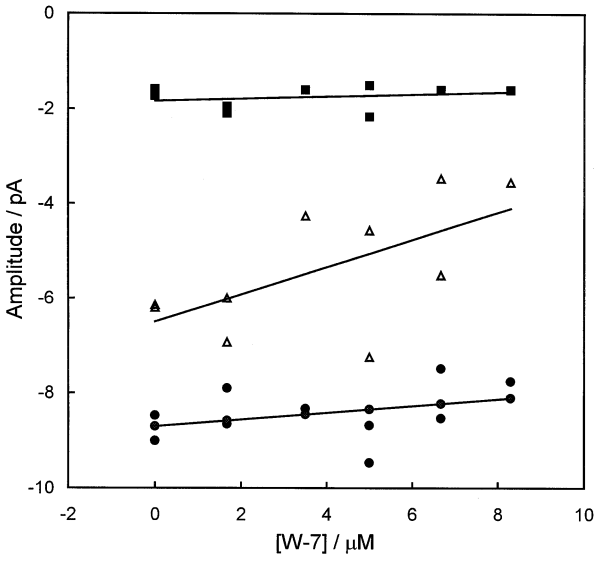

Fig. 5. Effect of W-7 on amplitudes of open, midstate and cluster states in symmetrical 1 μM Ca^{2+}. The current amplitudes were derived from HMM analysis (using Option #2). The states are: (●) open state; (△) cluster states consisting of a group of sparsely populated levels; (■) midstate. The lines show linear fits to the data. Experiments 31w7, 277w7 and dc239.

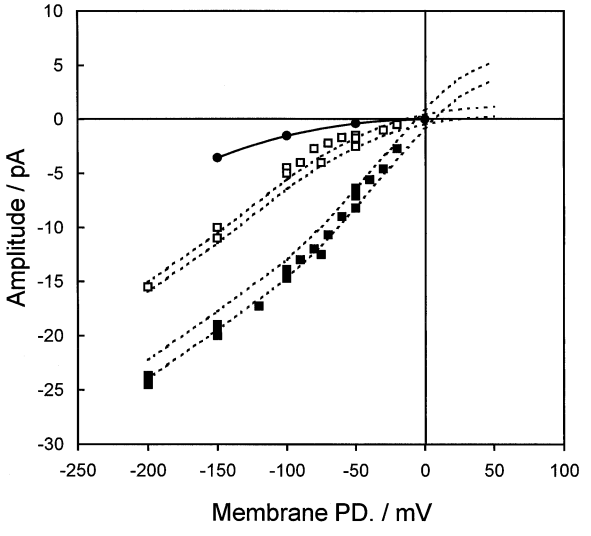

Fig. 6. The current-voltage characteristics of open (■) and midstate (□) in symmetrical 1 mM Ca^{2+} and at either 20 or 47 μM W-7, compared with control, shown as (dotted line) 95% confidence limits for polynomial regression (*data not shown*). Also shown in the current-voltage characteristics of new state induced by TFP. (●, *see* text), in symmetrical 1 mM Ca^{2+} Experiments 4#3850, dc100 and dc239.

The W-7 dependence of the mean durations of different conductance states (Fig. 7*B*) shows that W-7 has an effect only on the main state, causing a reduction in mean duration. The transition matrix produced by HMM (*not*

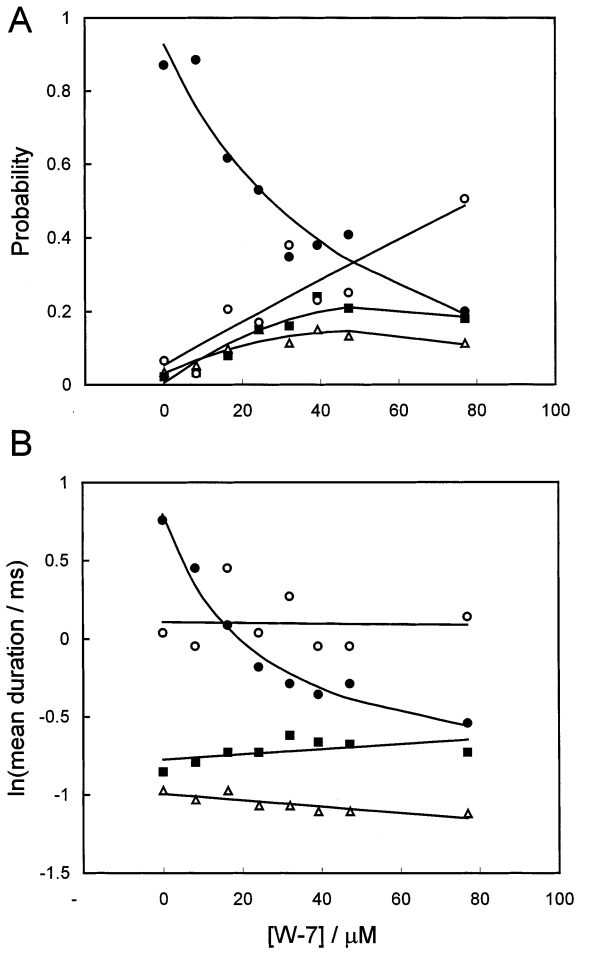

Fig. 7. Effect of W-7 on channel gating kinetics derived from HMM analysis (using Option #2, assuming four levels) expressed as level probability (*A*) and mean level duration (*B*). The levels are: (○) closed; (△) cluster; (■) midstate and (●) open. The channel was in symmetrical 1 mM Ca^{2+} at a membrane PD of −50 mV. Experiment dc239 shown here gave similar results to experiment 67W7.

shown) indicates that W-7 increases all the exit rates from the open state in the same proportion, and this increase is the cause of the reduction in mean duration noted above.

The frequency distributions of the open and substate durations were well fitted single exponentials (Tyerman *et al.*, 1992, and our data, *not shown*). The closed durations however have more than two exponential components, indicating more than two closed states. The frequency distributions of closed durations in the absence of W-7 and in 6.7 μM are shown in Fig. 8 for the channel of Fig. 3, using the scales suggested by Sigworth and Sine (1987). In such a plot individual exponential components show as peaks in the distribution, and in this example there would be at least two such components. W-7 has no effect on the distribution, showing that it has no effect on the closed state conformations.

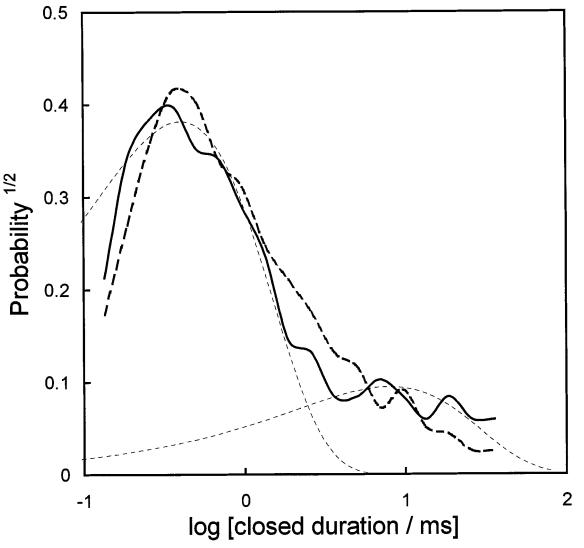

Fig. 8. Effect of W-7 on the probability distribution of closed times in 1 μM Ca^{2+} shown using the scaling suggested by Sigworth and Sine (1987) (Experiment 67w7 shown here is representative of five experiments). The W-7 concentrations are: (solid line) zero; (thick dashed line) 6.7 μM. The closed durations have at least two exponential components (shown by the dotted lines) which produce the overlapping peaks in the distribution.

Analysis of Flicker Block by TFP

Amplitude Histograms

Figure 9*A* shows the maximum likelihood amplitude histogram, generated by HMM, of a C-maxi-K channel in an inside-out patch with membrane PD of −50 mV in symmetric 150 mM KCl plus 1 mM $CaCl_2$. The histograms shown correspond to 0, 8 and 16 μM TFP. At −50 mV, 8 μM TFP reduces mean current to 0.37 of control (*data not shown*). Figure 9*A* shows that this is the combined result of a small decrease in amplitude and a pronounced decrease in open state probability. Figure 9*B* shows the mean duration verses amplitude for the maxi-K channel, generated by EVPROC, in the presence and absence of TFP, at −50 mV. TFP decreases both the mean open time and the mean closed time, while the substate durations are relatively unaffected.

In contrast to the effect of W-7, TFP did not alter the probabilities of midstate or cluster state(s) relative to the open state. At membrane PDs more negative than −100 mV the decrease in open state probability was absorbed by a new, TFP-induced substate. At −50 mV the substate could not be resolved from the closed state so that the decrease on open state probability seemed to be absorbed by a closed state component (Fig. 10).

Five- and Six-state Analysis

Figure 10 shows a portion of the amplitude histogram near the closed state, for 8 μM TFP, at different membrane PDs. The arrows above the plots show a level consistently chosen by HMM in multistate analysis, representing a new substate evoked by TFP, whose current-voltage curve is shown in Fig. 6.

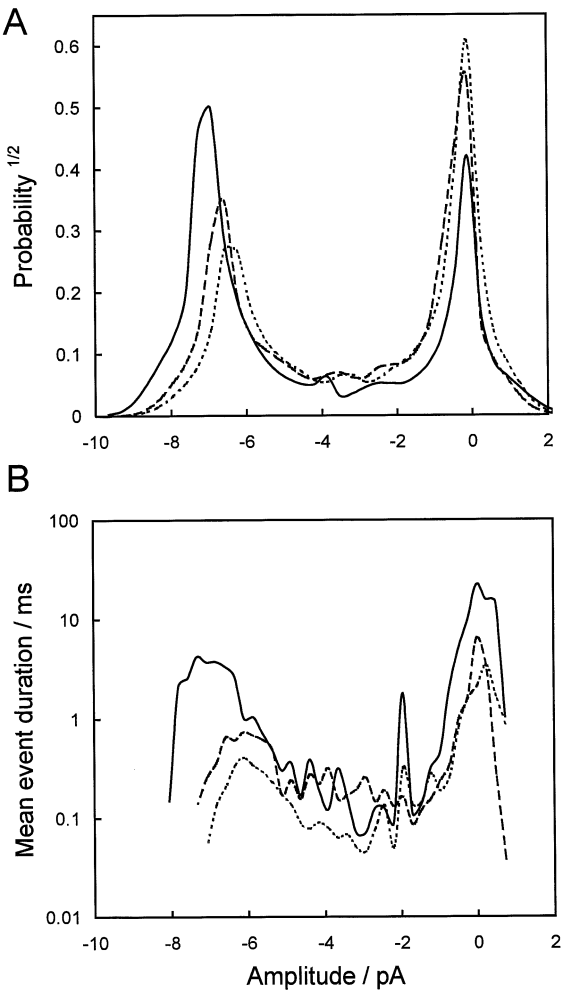

Fig. 9. Effect of TFP on the channel kinetics at −50 mV in 1 mM Ca^{2+}. The W-7 concentrations are: (solid line) zero; (dashed line) 8 μM; (dotted line) 16 μM. (*A*) the amplitude histogram from HMM analysis (Option #6), (*B*) mean duration at each level from EVPROC analysis. Experiment dc327 shown here gave a similar result to experiment cd1011 except the latter did not show the peak in part B at −2 pA.

Although at −50 mV TFP had no effect on the substate levels, it did, unlike W-7, alter the closed time frequency distribution produced by EVPROC. Figure 11 shows this frequency distribution of closed times generated by EVPROC. The scaling is the same as that used in Fig. 8 except that the data are normalized for record duration rather than event number. At −50 mV TFP causes a large increase in the frequency of closed events with an exponential time constant of approximately 1 msec. This additional TFP component in the closed time distribution at −50 mV is presumed to arise from the new substate which at more negative membrane PDs is more

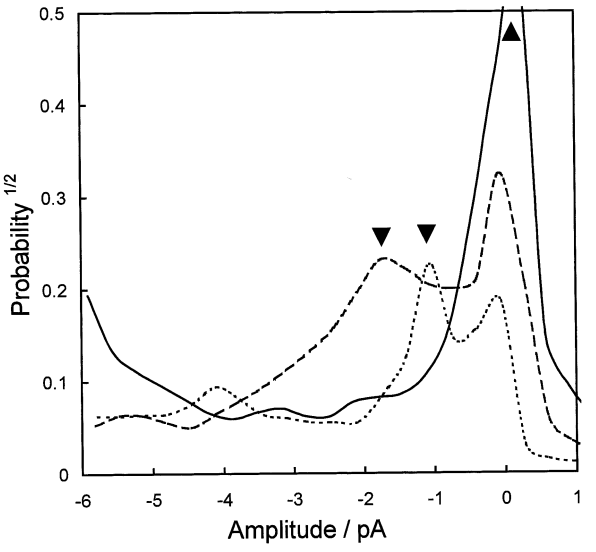

Fig. 10. Detail of channel amplitudes near the closed level showing the effect of membrane PD on the amplitude distributions in 8 μM TFP and in 1 mM Ca^{2+} over a range of membrane PDs. The membrane PDs are: (solid line) −50 mV; (dotted line) −100 mV; (dashed line) −150 mV. The peaks corresponding to the TFP induced substate are labeled indicated by the arrows. Experiment dc327 shown here gave a similar result to experiment dc320.

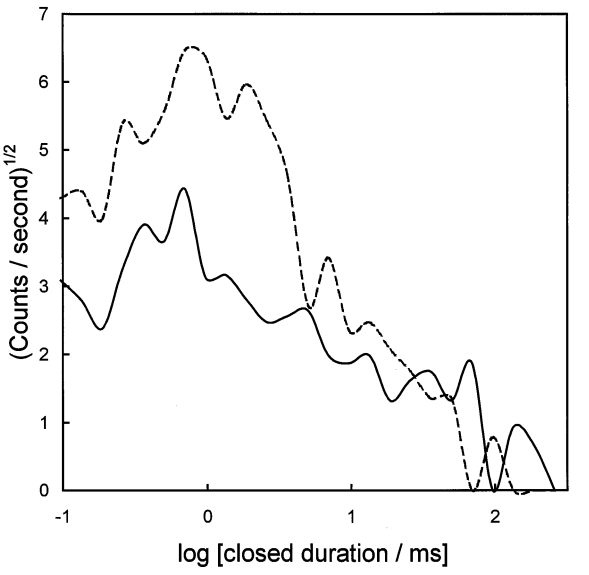

Fig. 11. Effect of 8 μM TFP in 1 mM Ca^{2+} on closed time frequency distributions at −50 mV. The concentrations of TFP are: (solid line) control; (dotted line) 8 μM. Both distributions have been normalized by their record length to allow direct comparison. Normalizing the frequency distributions by record length rather than event number more clearly reveals how TFP increases the number of events near 1 msec. Experiment dc327 shown here gave similar results to experiment cd1011.

clearly distinguished from the closed state (Fig. 10). The mean duration for this substate derived from HMM is 0.53 msec. This substate also seems to be the reason for the apparent reduction in mean closed time.

At membrane PDs larger than −100 mV the TFP-induced substate is partially resolved from the closed state and the increase in closed frequencies is less pronounced than at −50 mV (*data not shown*). The residual effect of TFP on closed frequencies at −100 mV may reflect ''spillage'' of ~30% of the nearby TFP-induced substates as neither EVPROC nor HMM could discriminate absolutely between the baseline and this substate. We are not able to rule out the alternative explanation, that TFP does alter the closed state distribution as well as introducing substates, but there is no need for the additional assumption it involves.

Effects of Calmodulin on Channel Activity and W-7 Block

When CAM was added to partly activated channels in 0.1 μM, 1 μM or 1 mM Ca^{2+}, there was no increase in open probability or in amplitude (*data not shown*). In the presence of W-7, 90 nM CAM relieved the block to some degree, at concentrations obviously too low for the CAM to titrate the W-7 present. In two experiments (*not shown*) CAM reversed the effect of W-7 on the amplitude distributions and mean substate durations. Therefore CAM appears to enhance channel activity by competitively antagonizing W-7 inhibition rather than by separate CAM-dependent activation mechanism.

Analysis of Ca^{2+} Activation

The Ca^{2+}-activation kinetics of the C-maxi-K channel were studied in detail in a previous paper (Laver & Walker, 1991). It was found that P_O increased over the range 0.1–10 μM and that this was mediated by a decrease in channel closed durations. Mean open duration of C-maxi-K channels was not significantly affected by [Ca^{2+}] over the range 0.1 μM to 1 mM. However, Laver and Walker (1991) did not investigate the effects of Ca^{2+}-activation on the substate kinetics, which is used in this study to distinguishing the mode of action of channel.

Amplitude histograms generated by EVPROC (*not shown*) of partially activated C-maxi-K channels in low [Ca^{2+}] show a relatively large closed level probability. There did not appear to be any differences in the substate probabilities (relative to the main open level) compared to fully activated channels over the PD range −50 to −150 mV. Thus it appears that these channels are Ca^{2+}-activated from a fully closed state.

Four-state analysis

HMM was used to analyze the Ca^{2+}-activation kinetics of single C-maxi-K channels from three patches. In

Table. Effects of channel regulators on C-maxi-K channel kinetics

	Main State	Midstate/substates	Closed state/s
Decreasing $[Ca^{2+}] < 10$ μM	Marginal reduction in mean duration Reduces probability	Mean duration unchanged Probability reduced in proportion with main state	Increases mean duration by intoducing long closures Increases probability relative to the main state
Increasing [W-7]	Reduces duration Reduces probability	Mean duration unchanged Increases probability relative to the main state	Mean duration unchanged Increases probability relative to the main state
Increasing [TFP]	Reduces duration Reduced probability	Induces new substrate	Probably unaffected

agreement with previous findings, the relatively low P_o at low $[Ca^{2+}]$ was mediated by a longer mean closed duration and a larger closed state probability. In addition, the substate analysis revealed that the probability and amplitude of the mid state, relative to that of the open state was similar in partially and fully activated channels. In one experiment, the gating kinetics of a C-maxi-K channel were measured at both 10 μM and 1 mM cytoplasmic Ca^{2+}. In 1 mM Ca^{2+} the probabilities of the open state and mid state were 0.74 and 0.031 respectively (a ratio of 0.042). For the same channel, only partly activated in 10 μM Ca^{2+} the probabilities of the open state and mid state were 0.05 and 0.0037 respectively (a ratio of 0.077). A ~30% blockade of the channel was induced by the presence of 1 mM Ca^{2+} (Laver, 1992) so that current levels at 10 μM and 1 mM Ca^{2+} could not be compared directly. However, the ratio of current amplitudes of the open state and the mid state at low and high $[Ca^{2+}]$ were both 0.41 suggesting that this subconductance state was not affected by the Ca^{2+}-activation site of the channel *per se*.

Discussion

Effects of W-7

The results and analysis presented above make it clear that W-7 has only a small effect on the conduction mechanism of the *Chara* maxi-K channel: it does however markedly affect the gating mechanism. W-7 increases the exit rates from the open state to the closed state and substates, which remain populated in the same proportion as in its absence. This is most easily understood in rate theory terms as an increase in the potential energy of the open state without any change in the activation energies of the transitions between it and the other states, whether substates or closed states. Since W-7 alters the open state duration it must bind to the open state; conservation of energy (which forbids equilibrium cycles) then requires that it also binds to closed and midstates. At high concentrations of W-7 the closed states observed are largely closed-and-bound-to-W-7. It is of interest that the closed state durations are not altered by W-7 binding.

The only other study of the effects of W-7 on Maxi-K channel kinetics is that of Kihira *et al.* (1990) on the A-Maxi-K channel of rat myometrium. The chief effect reported was a reduction of the longer of the two components of the open time distribution, and this is obviously compatible with our finding. The short time constant component in their open time distribution may well represent a substate or substates corresponding to the cluster of states in the C-Maxi-K channel since their analysis could not distinguish between these substates and the main open state.

The voltage-dependence of W-7 block would suggest, according to the Woodhull (1973) model, that it binds at a site within the transmembrane electric field, although we cannot rule out the possibility that other voltage-dependent factors such as current could regulated W-7 binding as is found for the binding of charybdotoxin (Park & Miller, 1992) to A-maxi-K channels.

Interaction between Ca^{2+} and W-7

Cytosolic Ca^{2+} causes a marked reduction in the potency of the W-7 block, which indicates an interaction between Ca^{2+} and W-7 at the channel protein. This interaction is weaker than that expected from direct competition since high $[Ca^{2+}]$ does not totally abolish W-7 binding. This result also indicates that Ca^{2+} and W-7 can simultaneously bind to the channel. The fact that inhibition of W-7 binding by Ca^{2+} saturates at concentrations less than 10 μM means that the Ca^{2+} binding site has similar affinity as the sites responsible for Ca^{2+}-activation of the channel (~1 μM, Laver & Walker, 1991). It is tempting then to speculate that W-7 competes with Ca^{2+} binding at the Ca^{2+}-activation site. However, this hypothesis is inconsistent with several other observations. While Ca^{2+} reduces the potency of W-7 the reverse is not true: the inhibiting effect of W-7 is not simply a reversal of Ca^{2+}-activation (*see* Table). Though we have not carried out

detailed measurement of the effect of W-7 on the Ca^{2+}-activation of the C-maxi-K channel, Kihira *et al.* (1990) have found that W-7 does not antagonize calcium-activation of the rat myometrium channel. Thus it appears that W-7 is acting on a high affinity Ca^{2+} site that is not essential for activation. There remains a possibility that the long, W-7 induced channel closures we observed at 1 μM Ca^{2+} could result from W-7 displacing Ca^{2+} from the activation site since Ca^{2+}-activation kinetics also involves long closures (*see* Table).

Interaction between Ca^{2+} and Calmodulin

We have detected no effect of added CAM on the C-Maxi-K channel in excised patches at 0.1 μM [Ca^{2+}]. Katsuhara and Tazawa (1992) reported the same lack of effect on normal channel activity in *Nitellopsis* tonoplast C-Maxi-K channels. Their results, however, were obtained in high [Ca^{2+}] which may have obscured any CAM effect. Further, the stimulating effect of added CAM is often difficult to demonstrate in membrane preparations, unless steps are added to the isolation procedure that remove endogenous CAM (Evans *et al.,* 1992; Rasi-Caldogno *et al.,* 1993).

In our experiments, spinach CAM showed an unexplained ability to relieve the effect of low W-7 concentrations, as it did in those of Bethke and Jones (1994) and of Weiser *et al.,* (1991) on the SV channel. The latter argued that this effect of *Chenopodium* CAM was evidence for the role of CAM in normal activation, particularly since bovine brain CAM was much less effective. Our results suggest that CAM may not be a part of normal activation.

While we have not tried the effect of brain CAM in our system, we do not see any of these experiments as conclusive, but as raising complex questions of three-way interaction.

Effects of TFP

Although TFP produces a flicker-block superficially similar to that produced by W-7, it is found to generate a new low-conductance state distinctly different from any seen in the native channel or under the influence of W-7. Thus, when substates are included in the analysis TFP and W-7 are seen to have kinetically distinct actions on the channel. We propose that the effect of TFP is simply to reduce the open-state conductance to that of the new substate.

Investigators of the A-Maxi-K channel, using heavy filtering and half-amplitude analysis, have not found any difference between the actions of TFP and W-7 (Kihira *et al.,* 1990) or between those of TFP and other neuroleptics (McCann and Welsh, 1987); it is clear that we would not have done so in the present case if we had used similar substate-insensitive methods of analysis. The substate created or promoted by TFP in our case would have been included in the closed state in McCann and Welsh's analysis, and this could easily have led to their conclusion that TFP blocked the channel. The analysis used by Kihira *et al.* (1990) was also incapable of distinguishing between closed state, and midstate and TFP-state, so that they could not have distinguished between W-7 and TFP actions. Thus these earlier reports are not inconsistent with our findings.

The concentration dependence of TFP inhibition suggests that high [TFP] totally abolishes the open state. Thus it appears that the substate represents times when TFP is bound and full opening represents times when TFP is not. Once this explanation is accepted, it is clear that TFP, like W-7, does not affect the true closed state of the channel.

Conclusions

In the present investigation we have shown:

(1) that W-7 and TFP interact with the channel in ways that do not simply reverse the effect of Ca^{2+} in activating the channel: it is clear that both W-7 and TFP reduce residence times in the (fully) open state, and appear to have no effect on the closed states, while Ca^{2+} alters the distribution of closed states; and

(2) that TFP and W-7 differ in their detailed kinetic effects, so can hardly be operating by a common mechanism such as inactivation of Ca-CAM.

This is the first investigation of the effects of CAM antagonists on a Maxi-K channel that includes substates in the analysis, so that we are the first to be able to differentiate the modes of action of W-7 and TFP in spite of the broad similarity of their effects in producing flicker-block. We conclude from this difference that at least one of W-7 and TFP binds directly to the channel, not to a putative Ca-CAM complex, and that most probably both bind directly to the channel. Similar conclusions on different grounds have been reached by McCann and Welsh (1987) and by Kihira *et al.* (1990).

Thus the actions of the CAM antagonists W-7 and TFP provide no evidence for CAM-activation of the C-Maxi-K channel, a conclusion that agrees with that of McCann and Welsh (1987) and of Kihira *et al.* (1990) for the A-Maxi-K channel, though based on different arguments. The postulated CAM-activation of the plant vacuolar SV channel is seen not to be well supported by the experiments to date and needs a detailed kinetic investigation.

We suggest that a substate-sensitive analysis of the effects of CAM antagonists on the A-Maxi-K channel will reveal analogous differences in their modes of action on gating in that channel also, and strengthen the evidence against its calcium-activation being CAM-mediated.

Calmodulin antagonists may be useful probes of channel gating mechanisms, but we join the many voices urging that their effects on channels should not be easily accepted as evidence for CAM itself activating them. Appropriate evidence for CAM activation can be obtained—e.g., as it was for immuno-affinity-purified cyclic-GMP-gated channels by Hsu and Molday (1994).

This work was supported by grants to N.A. Walker from the Australian Research Council and the University of Sydney; D.R. Laver was supported by a Senior Research Fellowship from the Australian Research Council.

References

Antkowiak, B., Kirshfeld, K. 1992. Enfurane is a potent inhibitor of high conductance calcium-activated potassium channels of *Chara australis. FEBS Lett.* **313:**281–284

Barrett, J.N., Magelby, K.L., Pallotta, B.S. 1982. Properties of single calcium-activated potassium channels in cultured rat muscle. *J. Physiol.* **331:**211–230

Bethke, P.C., Jones, R.L. 1994. Ca^{++}-calmodulin modulates ion channel activity in storage protein vacuoles of barley aleurone cells. *The Plant Cell.* **6:**277–285

Blatz, A.L., Magleby, K.L. 1987. Calcium-activated potassium channels. *Trends in Neurological Science* **10:**463–467

Chung, S.H., Moore, J.B., Xia, L.G., Premkumar, L.S., Gage, P.W. 1990. Characterization of single channel currents using digital signal processing techniques based on Hidden Markov Models. *Phil. Trans. Roy. Soc.* Series B **329:**265–285

Chung, S.H., Krishnamurthy, V., Moore, J.B. 1991. Adaptive processing techniques based on hidden Markov models for characterizing very small channel current buried in noise and deterministic interferences. *Phil. Trans. Roy. Soc.* Series B **334:**357–384

Colquhoun, D., Sigworth, F.J. 1983. Fitting and statistical analysis of single-channel records. *In:* Single-Channel Recording. B. Sakmann and E. Neher, editors. pp. 191–263. Plenum Press, New York

Evans, D.E., Askerlund, P., Boyce, J.M., Briars, S.A., Coates, D., Coates, J., Cooke, D.T., Theodoulou, F.L. 1992. Studies on the higher-plant calmodulin-stimulated ATPase. *In:* Transport and Receptor Proteins of Plant Membranes. D.T. Cooke and D.T. Clarkson, editors. pp. 39–53. Plenum Press, New York

Hedrich, R., Neher, E. 1987. Cytoplasmic calcium regulates voltage-dependent ion channels in plant vacuoles. *Nature* **329:**833–836

Hidaka, H., Sasaki, Y., Tanaka, T., Endo, T., Ohno, S., Fujii, Y., Nagata, T. 1981. *N*-(6-aminohexyl)-5-chloro-1-naphthalenesulfonamide, a calmodulin antagonist, inhibits cell proliferation. *Proc. Natl. Acad. Sci.* (USA) **78:**c4354–4357

Hinrichsen, R.D., Burgess-Casler, A., Soltvedt, B.C., Hennessey, T., Kung, C. 1986. Restoration by calmodulin of a Ca^{++}-dependent K^+ current missing in a mutant of *Paramoecium. Science* **232:**503–506

Hsu, Y.T., Molday, R.S. 1994. Interaction of calmodulin with the cyclic-GMP-gated channel of rod photoreceptor cells: modulation of activity, affinity purification and localization. *J. Biol. Chem.* **269:**29765–29770

Kamiya, N., Kuroda, K. 1957. Cell operation in *Nitella.* I. Cell amputation and effusion of the endoplasm. *Proc. Japan. Acad.* **33:**149–152

Katsuhara, M., Tazawa, M. 1992. Calcium-regulated channels and their bearing on physiological activities in Characean cells. *Phil. Trans. Roy. Soc.* (London). Series B **338:**19–29

Kihira, M., Matsuzawa, K., Tokuno, H., Tomita, T. 1990. Effects of calmodulin antagonists on calcium-activated potassium channels in pregnant rat myometrium. *Brit. J. Pharmacol.* **100:**353–359

Klaerke, D.A., Petersen, J., Jorgensen, P.L. 1987. Purification of Ca^{--}-activated K^+-channel protein on calmodulin affinity columns after detergent solubilization of luminal membranes from outer renal medulla. *FEBS Lett.* **216:**211–216

Kourie, J.I., Laver, D.R., Junankar, P.R., Gage, P.W., Dulhunty, A.F. 1996. Two types of chloride channel in sarcoplasmic reticulum of rabbit skeletal muscle. *Biophys. J.* **70:**202–221

Laver, D.R. 1990. Coupling of K^+-gating and permeation with Ca^{2+}-activated K^+ channel in *Chara australis. J. Membrane Biol.* **118:**55–67

Laver, D.R. 1992. Divalent cation block and competition between divalent and monovalent cations in the large-conductance K^+ channel from *Chara australis. J. Gen. Physiol.* **100:**269–300

Laver, D.R., Walker, N.A. 1987. Steady-state voltage-dependent gating and conduction kinetics of single K^+ channels in the membrane of cytoplasmic drops of *Chara australis. J. Membrane Biol.* **100:**31–42

Laver, D.R., Walker, N.A. 1991. Activation by Ca^{2+} and block by divalent ions of the K^+ channel in the membrane of cytoplasmic drops from *Chara australis. J. Membrane Biol.* **120:**131–139

Lühring, H. 1986. Recording of single K^+ channels in the membrane of cytoplasmic drop of *Chara australis. Protoplasma* **133:**19–27

McCann, J.D., Welsh, M.J. 1987. Neuroleptics antagonize a calcium-activated potassium channel in canine airway smooth muscle. *J. Gen. Physiol.* **89:**339–352

Okihara, K., Ohkawa, T.-a., Kasai, M. 1991. Effects of calmodulin on Ca^{++}-dependent Cl^--sensitive anion channels in the *Chara* plasmalemma: a patch-clamp study. *Plant Cell Physiol.* **34:**75–82

Onozuka, M., Furuichi, H., Kishii, K., Imai, S. 1987. Calmodulin in the activation process of calcium-dependent potassium channel in *Euhadra* neurones. *Comp. Biochem. Physiol.* **86***A*:589–593

Park, C.S., Miller, C. 1992. Interaction of charybdotoxin with permeant ions inside the pore of a K^+ channel. *Neuron* **9:**307–313

Rasi-Caldogno, F., Carnelli, A., De Michaelis, M.I. 1993. Controlled proteolysis activates the plasma membrane Ca^{++} pump of higher plants. *Plant Physiol.* **103:**385–390

Roufogalis, B.D. 1982. Specificity of trifluoperazine and related phenothiazines for calcium-1 binding proteins. *In:* Calcium and Cell Function. Vol. 3. W.Y. Chung, editor. pp. 129–159. Academic Press, New York

Sakano, K., Tazawa, M. 1986. Tonoplast origin of the membrane of cytoplasmic droplets prepared from *Chara* internodal cells. *Protoplasma* **131:**247–249

Shatzman, R.C., Raynor, R.L., Kuo, J.F. 1983. *N*-(6-aminohexyl)-5-chloro-1-naphthalenesulfonamide (W-7), a calmodulin antagonist, also inhibits phospholipid-sensitive calcium-dependent protein kinase. *Biochim. Biophys. Acta.* **755:**144–147

Sigworth, F.J., Sine, S.M. 1987. Data transformations for improved display and fitting of single-channel dwell time histograms. *Biophys. J.* **52:**1047–1054

Tyerman, S.D., Terry, B.R., Findlay, G.P. 1992. Multiple conductances in the large K^+ channel from *Chara corallina* shown by a transient analysis method. *Biophys. J.* **61:**736–749

Weiser, T., Bentrup, F.-W. 1993. Pharmacology of the SV channel in the vacuolar membrane of *Chenopodium rubrum* suspension cells. *J. Membrane Biol.* **136:**43–54

Weiser, T., Blum, W., Bentrup, F.-W. 1991. Calmodulin regulates the Ca^{++}-dependent slow-vacuolar ion channel in the tonoplast of *Chenopodium rubrum* suspension cells. *Planta* **185:**440–442

Williamson, R.E., Ashley, C.C. 1982. Free Ca^{++} and cytoplasmic streaming in the alga *Chara. Nature* **296:**647–651

Woodhull, A.M. 1973. Ionic blockage of sodium channels in nerve. *J. Gen. Physiol.* **61:**687–708